JMEPEG (2007) 16:800–806
DOI: 10.1007/s11665-007-9149-5

1059-9495/$19.00

Study of Surface Morphology in Welds of Ti-5Ta-1.8Nb Alloy Exposed to 11.5 M Boiling Nitric Acid

Arup Dasgupta, T. Karthikeyan, S. Saroja, V.R. Raju, M. Vijayalakshmi, R.K. Dayal, and V.S. Raghunathan

(Submitted July 29, 2005; in revised form June 23, 2006)

This article presents the study on corrosion behavior of welds of a Ti-5%Ta-1.8%Nb alloy—a candidate material for reprocessing plant, where it is exposed to highly concentrated (11.5 M) and boiling nitric acid. The corrosion rates of Ti-Ta-Nb alloy in wrought condition have been established earlier to be low (0.26 mpy in liquid). The successful use of this material crucially depends on the behavior of its welds. Evaluation of corrosion rates of the welds in boiling nitric acid in the liquid, vapor, and condensate phases showed that the rates were low, <1 mpy and were comparable or less than those of the base metal. Since microstructure plays an important role in governing the corrosion rate, the microstructures in as-welded and nitric acid exposed conditions were studied. The alloy in "as-welded" state has a martensitic structure, which is microstructurally and microchemically homogeneous. Examination of the corroded surface showed the formation of a protective film, which acts as a barrier to dissolution of Ti after the initial high dissolution. The film was found to be ruptured at regions where Si-rich particles were embedded during surface preparation. The present studies have shown that the Ti-Ta-Nb welds show good corrosion resistance in all three phases of nitric acid and the alloy can be employed in highly oxidizing medium.

Keywords microstructure, nitric acid, three phase corrosion, Ti alloy, weld

1. Introduction

Reprocessing of spent fuel from nuclear reactors requires its dissolution in boiling nitric acid, which is a highly oxidizing medium. Zirconium as well as titanium and their alloys have been reported to possess excellent corrosion resistance in nitric acid even in the presence of fission products with high-redox potential (Ref 1). Their excellent corrosion resistance is due to a continuous, stable, highly adherent and protective (or passive) oxide film. The nature, composition, and thickness of the protective surface oxide that forms on titanium alloys depend on environmental conditions. In most aqueous environments, Ti forms TiO_2, Ti_2O_3, or TiO (Ref 2). The oxidation potential of boiling HNO_3 is high enough to yield TiO_2 (rutile) though it is possible to form chemically unstable Ti_2O_3 (Ref 3). Titanium has excellent corrosion resistance in liquid nitric acid, but under relatively weak oxidizing conditions such as in the vapor and condensate phases, has been reported to exhibit a higher corrosion rate (Ref 4). The corrosion resistance of titanium in condensed HNO_3 can be improved by alloying with refractory metals such as Tantalum (Ta) and Niobium (Nb). Ta and Nb have metallic ion size similar to that of titanium and lowers Ti solubility in HNO_3 by stabilizing the passive oxide film (Ref 5). Addition of about 5 wt.% Ta to Ti reduces the corrosion by almost 4.5 times, while addition of up to 1.8 wt.% Nb to Ti-5 wt.% Ta enhances the corrosion resistance almost 1.5 times. Hence, Ti-5%Ta-1.8%Nb alloy is a potential candidate material for structural applications such as vessels for dissolvers and evaporators in nuclear fuel reprocessing plants (Ref 5, 6).

The physical metallurgy database for this alloy generated in our laboratory (Ref 7, 8) based on x-ray diffraction and detailed transmission electron microscopy analysis classifies the alloy as two phase, containing hcp α and bcc β phases. The β transus of the alloy was evaluated (Ref 7) to be 870 °C. The corrosion rates of the wrought alloy with a predetermined thermomechanical treatment has been studied in our laboratory and established to be 0.26, 0.51, and 2.77 mpy in the liquid, vapor, and condensate phases, respectively (Ref 9).

Welding is an indispensable step in fabrication of any industrial component. The weldability of this alloy having identical properties of the wrought material described above has been assessed in our laboratory and established to be good. The results have been published in our earlier reports (Ref 10, 11). The successful use of the new Ti-Ta-Nb alloy in highly oxidizing media would therefore depend on the corrosion behavior of its weldments. Hence, the corrosion behavior of the weld of Ti-5Ta-1.8Nb alloy has been investigated. This report presents the studies on corrosion of Ti-5Ta-1.8Nb alloy in boiling (117 °C) and concentrated (11.5 N) nitric acid in liquid, vapor, and condensate phases.

2. Experimental

Ti-5Ta-1.8Nb alloy, used in the present study was supplied by Nuclear Fuel Complex, Hyderabad, in the form of 12.5 mm ϕ cylindrical rods. The fabrication route for the alloy is discussed elsewhere (Ref 6). Its chemical composition is given in Table 1. Weldments of the Ti-Ta-Nb alloy were fabricated by

Arup Dasgupta, T. Karthikeyan, S. Saroja, V.R. Raju, M. Vijayalakshmi, R.K. Dayal, and **V.S. Raghunathan**, Materials Characterisation Group, Indira Gandhi Centre for Atomic Research, Kalpakkam 603 102, India. Contact e-mail: saroja@igcar.ernet.in.

Table 1 Composition of the alloy

Element	Ta, wt.%	Nb, wt.%	Impurities					Ti
			Fe, wt.%	O, ppm	N, ppm	C, ppm	H, ppm	
Content	4.39	1.94	0.0263	501.5	47	125	9	Balance

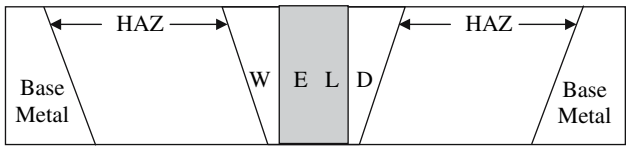

Fig. 1 Schematic of the weldment. The weld, heat affected zone (HAZ), base metal regions, and location of test coupons for corrosion studies (shaded region) are shown in the figure

manual GTAW (gas tungsten arc welding) process as per ASME section IX guidelines, the details of which are given elsewhere (Ref 11). The geometry of the weldment is shown in Fig. 1. The weld, heat affected zone (HAZ), and base metal regions are marked in the figure.

The weld region was sectioned along the middle, parallel to the weld centerline. The cross section was prepared by standard metallographic procedures. The weld surface was etched using a reagent comprising of 3 mL HF, 2 mL HNO_3, and 95 mL H_2O, to reveal its microstructure. Microstructural and microchemical characterization of the weld was carried out by Scanning Electron Microscopy (SEM) and energy dispersive x-ray spectroscopy (EDS) using a Philips XL-30 ESEM equipment.

The corrosion rates were measured in boiling nitric acid by standard practice similar to ASTM A262 practice C for AISI 304L SS (Ref 12), which is an accepted technique for evaluation of corrosion in Ti and Ti alloys (Ref 1, 4). Specimens of dimensions ~$10\times10\times2.5$ mm were cut from the weld region (shaded region in Fig. 1), excluding regions from the HAZ of the weldment. These specimen were polished up to 600 grit emery finish, cleaned with water and acetone and dried in hot air. These were then weighed up to an accuracy of 0.0001 g, before exposing them to the liquid, vapor, and condensate phases of 11.5 M boiling (117 °C) nitric acid. The experimental setup used is shown in Fig. 2, which is a modified version of the arrangement used by Furuya et al. (Ref 4). The specimens were exposed for a total period of 240 h. The ratio of volume of solution to the total specimen surface area in liquid, vapor, and condensate phases together was about 75 mL/cm^2. The design of the experimental setup ensured that the corrosion rate of the sample in condensate phase is not influenced by dissolved ions, since the solution condensing in the inner vessel was automatically siphoned out and replenished at regular intervals. However, in the liquid zone, corrosion rate is influenced by dissolved ions and the concentrated soluble titanium ions in the solution act as inhibitors (Ref 4). The change in weight and surface appearance were examined by removing the specimens after every 48 h. This test was repeated on two sets of samples to check the reproducibility of results. After completion of the test, corrosion rates in individual periods and average corrosion rate for five individual periods were calculated. It may be mentioned here that, any error in evaluation of corrosion rate arises due to

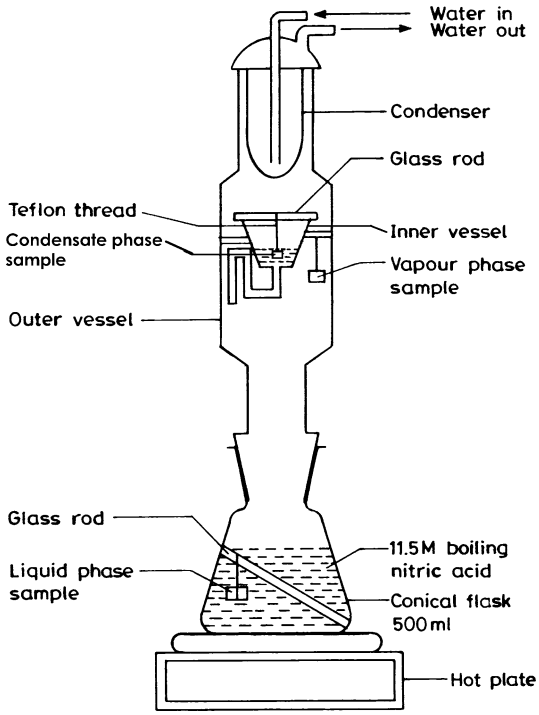

Fig. 2 Schematic of the experimental setup for corrosion tests in liquid, vapor, and condensate phases of nitric acid

measurement of surface area of small sized samples and small weight changes. The corroded surfaces were examined again by SEM to observe the change in surface characteristics due to exposure to boiling nitric acid.

3. Results and Discussion

3.1 Characterization of Microstructure in "As-welded" Condition

The secondary electron image from a typical region on the "as-welded" surface is shown in Fig. 3(a). The figure shows fine needle-like features of varying lengths characteristic of martensite (Ref 13). The microstructure was found to be uniform in the entire weld region. A typical energy dispersive x-ray (EDS) spectrum from the weld surface is superimposed on the micrograph in Fig. 3(a). The spectrum shows peaks corresponding to Ti-Kα, Nb-Lα, and Ta-Mα, typical of the Ti-5Ta-1.8Nb alloy (Ref 14). EDS spectra acquired from a large number of regions showed no microchemical heterogeneities across the weld surface, which is in agreement with the martensitic structure. The microstructure of the weld can therefore be summarized as a uniform martensitic structure with no microchemical inhomogeneities signifying a typical

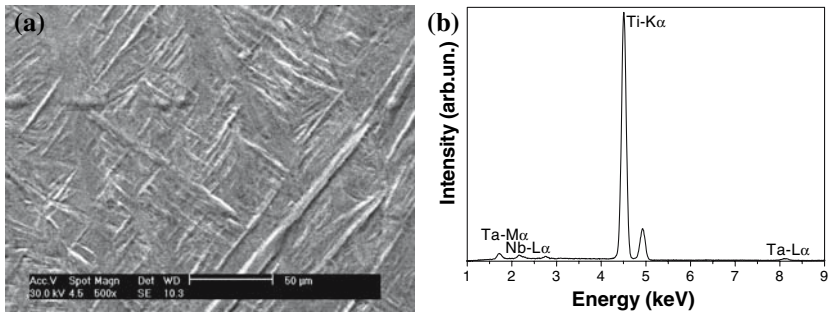

Fig. 3 (a) Secondary electron image of the weld surface showing a uniform martensitic structure; (b) EDS spectra from the weld showing the alloy constituents

Table 2 Corrosion rates of TiTaNb welds in hot and concentrated nitric acid after every 48 h of treatment in the liquid, vapor, and condensate phases; results of two sets of such readings and their overall average are shown

Where exposed	Corrosion rate after each period, mpy										Avg. corrosion rate, mpy
	48 h		96 h		144 h		192 h		240 h		
	1st set	2nd set	1st set	2nd set	1st set	2nd set	1st set	2nd set	1st set	2nd set	
Liquid	1.65	0.83	0.826	Nil	Nil	Nil	Nil	Nil	Nil	Nil	0.33
Vapor	Nil	Nil	Nil	Nil	Nil	Nil	Nil	1.46	Nil	2.92	0.44
Condensate	Nil	Nil	1.35	Nil	Nil	1.35	Nil	Nil	Nil	Nil	0.27

diffusionless transformation. This is in contrast to the microstructure of the base metal which consists of a distribution of fine β precipitates in an equiaxed α matrix (Ref 10, 11). A region from the weld alone (excluding sections from HAZ and base metal) was selected for the corrosion tests, the results of which are discussed below.

3.2 Evaluation of Corrosion Rates in Liquid, Vapor, and Condensate phases of 11.5 M Nitric Acid

Table 2 shows the corrosion rates evaluated from the weight loss of TiTaNb alloy weld in the three phases namely liquid, vapor, and condensate of boiling nitric acid after every 48 h period until 240 h. The average and measured data for two sets of experiments are shown. It is observed that the average corrosion rate is extremely low (<1 mpy) in each of the three phases. Comparing these values of corrosion rates with our earlier report (Ref 9), it can be said that they compare well with those for the wrought alloy (or base metal) in all the three phases (0.26 mpy in liquid, 0.51 mpy in vapor and 2.77 mpy in condensate). These results suggest that the corrosion resistance of the weld of Ti-Ta-Nb alloy is extremely good in all the three phases of 11.5 M boiling nitric acid and is similar to that of the base metal in the liquid and vapor phases and one order lower in the condensate phase. This property is an essential criterion for successful performance of the weld in highly oxidizing environment.

It can be seen from Table 2 that the corrosion rate in the liquid phase is relatively higher initially and reduces to very low values at longer times, whereas in vapor and condensate phases the behavior was different. No attempt has been made to deduce any trends due to limited data and the observed scatter in the data. However, it is observed that the average corrosion rate in all three phases is quite low with the condensate phase (0.27 mpy) showing the lowest.

It is well-known that astounding corrosion resistance of Ti is derived from the tenacious oxide film that develops on the surface when exposed to a highly oxidizing environment such as nitric acid. However, in a boiling concentrated (11.5 N) nitric acid medium, the initial kinetics of film growth is governed by a dynamic process of formation of the passive oxide film and dissolution of metallic Ti until the concentration of Ti ions in the medium inhibits further dissolution (Ref 15). Initially the dissolution is high when the material is exposed to the liquid medium, as is seen from the table. But once the oxide film is formed, its impervious nature inhibits further corrosion. Alloying elements such as Ta and Nb help to stabilize the passive oxide layer (Ref 16). Additionally, the dissolved Ti ions in solution act as inhibitors, which reduce the rate of further dissolution of Ti from the surface and hence the corrosion rate. This explains the observed behavior in the liquid phase.

The nature of protective oxide film that forms on the surface of Ti and its alloys is very sensitive to the environment (Ref 2). This could alter the characteristics of the film that forms during exposure to liquid, vapor, and condensate phases of nitric acid. It is reported (Ref 3, 4) that the oxide film that forms in liquid phase is more stable and protective as compared to that which forms in the vapor or condensate phases. The nature of the films is under study and is beyond the purview of this article. The less stable nature of film together with the absence of inhibition effect of dissolved Ti ions in vapor and condensate phases is expected to result in high-corrosion rates, in comparison to the liquid phase. However, the measured corrosion rates of 0.44 and 0.27 mpy in vapor and condensate phases, respectively, are not high, which suggests that the absence of the inhibiting effect of dissolved Ti ions in the liquid phase is compensated by other factors. The phase diagram (Ref 4) for the azeotropic mixture of nitric acid and water is shown in Fig. 4. It can be seen that concentration of nitric acid in the vapor phase is always lower than that in the liquid phase for concentrations

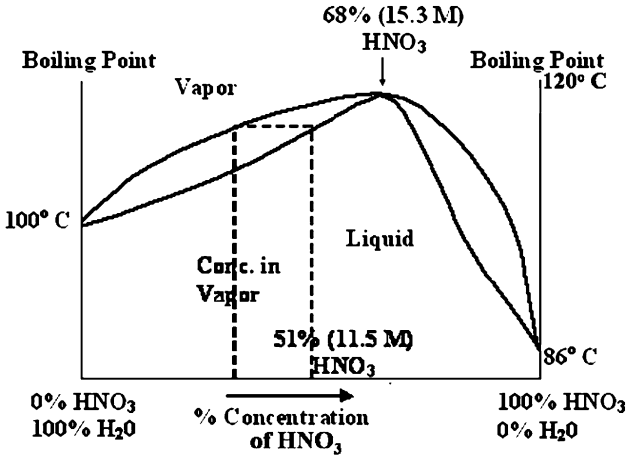

Fig. 4 Nitric acid-water phase diagram (Ref 4). The iso-concentration line corresponding to 115 M nitric acid, that in the vapor phase and the corresponding tie-line is also shown

below 68% (15.3 M); whereas the behavior is reversed for concentrations above 68%. In the present study 11.5 M nitric acid (~51% HNO_3) has been used. The low concentration of nitric acid is responsible for the low-corrosion rate in the vapor phase, which is comparable to that of liquid phase. The concentration of nitric acid in the condensate phase is also expected to be similar to that of vapor phase (Ref 4), which accounts for the low-corrosion rate. The above results showed that the observed corrosion behavior of Ti-Ta-Nb alloy in three phases of nitric acid is an interplay of different factors like nature of the protective film, inhibiting effect of dissolved Ti ions and concentration of nitric acid.

3.3 Analysis of Surface Morphology of Ti-Ta-Nb Alloy Exposed to Nitric Acid

The surface topography after exposure of the weld to hot and concentrated nitric acid in the liquid, vapor, and condensate phases are shown at identical magnifications in Fig. 5(a-c). The remnant marks of polishing with 600 grit abrasive seen as parallel elongated marks in the images are ignored. Close observation of the corroded surface showed the presence of discontinuities, cracks, and pits in all the three cases. This suggests that the film that formed was discontinuous and ruptured at few regions, which could have led to formation of cracks or large pits. The number density and distribution of these pits are similar in all three cases, which indicate their formation to a common origin. It is well-known that Ti or its alloys do not undergo pitting corrosion under similar experimental conditions of exposure.

The elemental x-ray maps from a region on the surface film of TiTaNb exposed to liquid phase of boiling and concentrated nitric acid is shown in Fig. 6. Figure 6(a) shows the secondary electron image of the selected region showing a "pit"-like feature marked as "P." The feature measures about 8 μm in length. Figure 6(b-e) show characteristic x-ray images of Ti-Kα, Ta-Mα, Nb-Lα, and Si-Kα, respectively. It is observed that there is a uniform distribution of Ta and Nb in the region. However, the x-ray maps of Ti and Si show a nonuniform distribution between the matrix and the pit-like feature. This could be due to the overlapping of Ta-Mα and Si-Kα peaks, since the energy difference is beyond the resolution of the

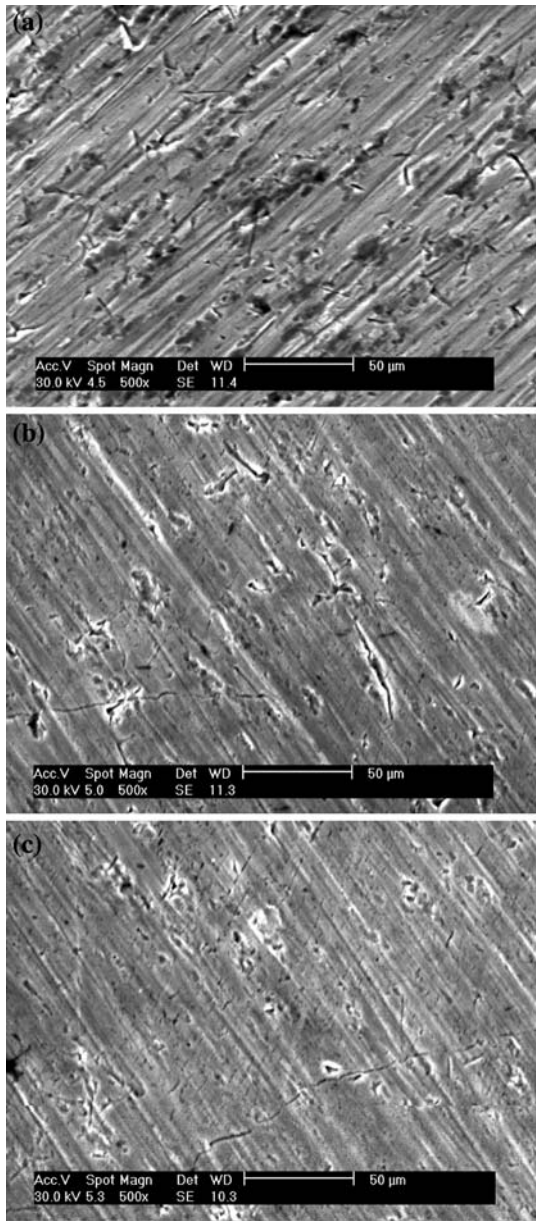

Fig. 5 Secondary electron images of the weld surface exposed to nitric acid in (a) liquid, (b) vapor, and (c) condensate phases

technique. However, the Ta-Lα peak used to resolve this ambiguity clearly shows that there is an enrichment of Si around the pit-like feature marked as "P" and that Ti is almost absent in these regions. These results suggest the presence of a Si-rich particle in the film, which may also be responsible for the observed rupture of the film in such regions. Such a behavior has been observed on a large number of regions on the surface. Figure 6(f) shows the secondary electron image of the cross section of this sample. From this micrograph, it is observed that the thickness of the passive oxide film on the weld surface is about 1 μm. Presence of particles projecting out of the film surface are also observed from this figure. The microchemistry of these particles analyzed using EDS showed the presence of a Si-rich phase. These results show that the embedded Si-rich particles are responsible for rupturing the otherwise continuous passive oxide film. It is possible that

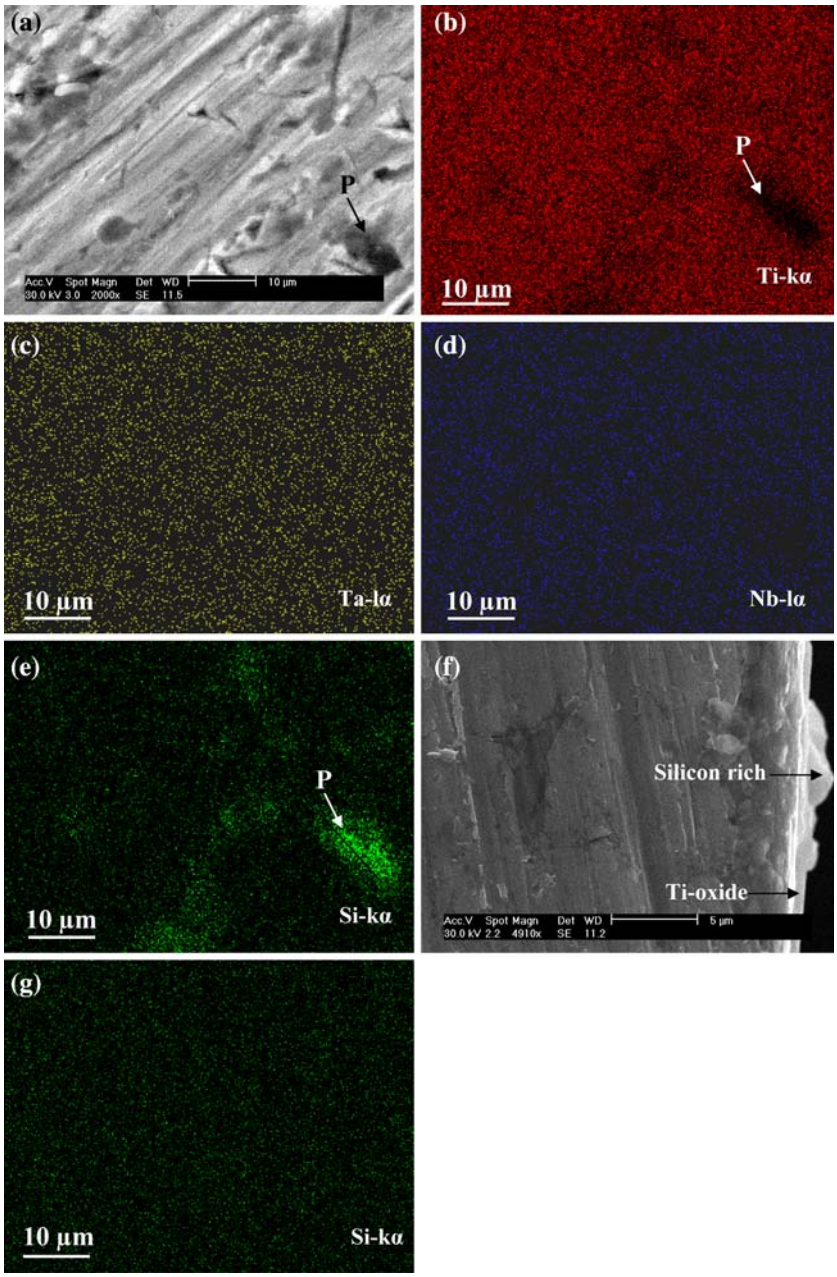

Fig. 6 (a) Secondary electron image of the surface of the weld exposed to liquid nitric acid, (b-e) x-ray images corresponding to Ti-Kα, Ta-Lα, Nb-Lα, and Si-Kα, respectively, for the area corresponding to (a); (f) Secondary electron image of the cross section of this sample; (g) x-ray image corresponding to Si-Kα for the as-welded surface area shown in Fig. 3(a)

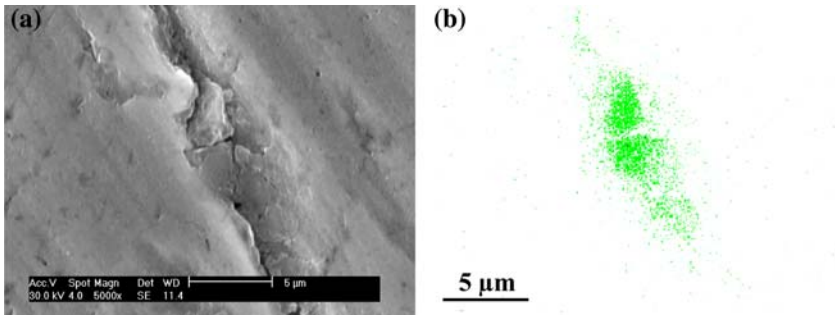

Fig. 7 (a) Secondary electron image of the oxide surface near a crack from a sample exposed to nitric acid condensate, (b) x-ray image corresponding Si-Kα of sample surface corresponding to (a) showing enrichment in Si near the center of the crack

the presence of these particles also alter the characteristics of the film to different extents when the weld is exposed to liquid, vapor, and condensate phases of nitric acid. The SiC particles may have been embedded in the soft Ti surface during the surface preparation for corrosion tests, which includes polishing with 600 grit emery paper.

In order to understand the nature of defect produced in the oxide film by the embedded SiC particle, a region of TiTaNb weld exposed to nitric acid vapors has been studied and results are shown in Fig. 7. Figure 7(a) and (b) show the secondary electron and x-ray image of such a region showing the presence of Si. From the figure it appears that two such particles are embedded in the region. Figure 7(a) reveals that the oxide film develops cracks on either side of these particles, which may be detrimental for the passive layer since nitric acid may penetrate through these cracks resulting in enhanced corrosion.

The above observation assumes importance in the context of industrial practice and the implication of the stability of passive oxide film, which determines the corrosion rate of the industrial component. It may be pointed out here that, the corrosion tests have been carried out under conditions chosen to resemble those of actual large-scale components such as tanks, pipes, tubes, etc., where little or no surface preparation may be possible in practice. The conditions of evaluation of corrosion rate also conform to the standard ones used for stainless steels and Ti alloys (Ref 12, 17, 18) as per ASTM Practice A262 tests. Thus, it can be said that if the presence of these foreign particles on the surface can be avoided or even minimized through chemical cleaning, the corrosion rates could have been still lower since passive film rupture could have been prevented. Hence, rupture of passive, protective film due to the presence of foreign particles, suggests the necessity to modify the procedure for cleaning of industrial components, where corrosion resistance is crucial to ensure long service life.

4. Conclusions

The corrosion resistance of welds of Ti-5Ta-1.8Nb alloy, a candidate material for structural applications in reprocessing plants has been established in liquid, vapor, and condensate phases of boiling (117 °C) and concentrated (11.5 N) nitric acid. The salient features of the study are as follows:

- The weld consists of a uniform martensitic structure with no microchemical heterogeneity in the "as-welded" condition.
- The welds exhibit a very low-corrosion rate (<1 mpy) in the liquid, vapor, and condensate phase of boiling 11.5 M nitric acid.
- The corrosion rates of welds are comparable to that of the base metal.
- The high-corrosion resistance is attributed to the presence of a protective oxide film, which acts as a barrier to dissolution of Ti after the initial dissolution. The time dependence of corrosion rate in the liquid phase is understood in terms of interplay between formation of protective oxide film and the dissolution of metal ions.
- Very low-corrosion rates in the vapor and condensate phases are understood in terms of lower concentration of nitric acid in these media.
- The corroded surface shows rupture of the protective oxide film at few regions due to the Si-rich particles that are embedded on the surface during surface preparation. Careful surface preparation is recommended to avoid this problem.

Acknowledgments

The authors gratefully acknowledge Dr. Baldev Raj, Director—Indira Gandhi Centre for Atomic Research and Dr. S.L. Mannan, Director—Materials and Metallurgy Group, IGCAR for the support and encouragement provided during the course of this work.

References

1. U.K. Mudali, R.K. Dayal, and J.B. Gnanamoorthy, Corrosion Studies on Materials of Construction for Spent Nuclear Fuel Reprocessing Plant Equipment, *J. Nucl. Mater.*, 1993, **203**, p 73–82
2. R.W. Schutz, *Corrosion Tests and Standards: Application and Interpretation*, ASTM Manual Series: MNL 20, R. Baboian, Ed., ASTM, Philadelphia, USA, 1995, p 493–506
3. K. Kiuchi, M. Hayashi, H. Hayakawa, M. Sakairi, and M. Kikuchi, "Fundamental Study of Controlling Factors on Reliability of Fuel Reprocessing Plant Materials used in Nitric Acid Solutions," A Poster Paper in Session: *Corrosion and Materials Selection, Proc. Fourth Int. Conf. on Nuclear Fuel Reprocessing and Waste Management*, RECOD '94, Vol. III, April 24-28, 1994, London
4. T. Furuya, J. Kawafuku, H. Satoh, K. Shimogori, A. Aoshima, and S. Takeda, Corrosion Testing Method for Titanium in Nitric Acid Environments, *ISIJ Int.*, 1991, **31**(2), p 189–193
5. K. Kiuchi, H. Hayakawa, Y. Takagi, and M. Kikuchi, "New Alloy Development for Fuel Reprocessing Plant Materials Used in Nitric Acid Solutions," A Poster Paper in Session: *Corrosion and Materials Selection, Proc. Fourth Int. Conf. Nuclear Fuel Reprocessing and Waste Management*, RECOD'94, Vol. III, April 24-28, 1994, London
6. K. Kapoor, V. Kain, T. Gopal Krishna, T. Sanyal, and P.K. De, High Corrosion Resistant Ti-5%Ta-1.8%Nb Alloy for Fuel Reprocessing Application, *J. Nucl. Mater.*, 2003, **322**, p 36–44
7. R. Mythili, V. Thomas Paul, S. Saroja, M. Vijayalakshmi, and V.S. Raghunathan, Study of Transformation Behavior in a Ti-4.4 Ta-1.9 Nb Alloy, *Mater. Sci. Eng.*, 2005, **A390**, p 299–312
8. T. Karthikeyan, A. Dasgupta, A.J. Khan, S. Saroja, M. Vijayalakshmi, D. Bhattecharjee, and V.S. Raghunathan, Study of Texture in a TiTaNb Alloy Using Electron Back Scattered Diffraction Technique, *Mat. Sci. Eng.*, 2005, **A393**, p 294–302
9. R. Mythili, A. Ravi Shankar, S. Saroja, V.R. Raju, M. Vijayalakshmi, R.K. Dayal, V.S. Raghunathan, and R. Balasubramaniam, Influence of Microstructure on Corrosion Behavior of Ti-5%Ta-1.8%Nb Alloy, *J. Mater. Sci.*, 2007, **42**(50), p 5924–5935
10. T. Karthikeyan, A. Dasgupta, S. Saroja, M. Vijayalakshmi, and V.S. Raghunathan, Studies on Weldability of Ti-5Ta-1.8Nb Alloy, *J. Nucl. Mat.*, 2004, **335**, p 299–301
11. T. Karthikeyan, A. Dasgupta, S. Saroja, and M. Vijayalakshmi, Weldability and Microstructural Variations in Weldments of Ti-5Ta-1.8Nb Alloy, *J. Mater. Eng. Perform. (ASM Intl.)*, 2005, **14**, p 241–248
12. "Standard Practices for Detecting Susceptibility to Intergranular Attack in Austenitic Stainless Steel," A262-86, Annual Book of ASTM Standards, Vol. 03.02, ASTM, 1986, p 1–18
13. F.J. Gil, M.P. Ginebra, J.M. Manero, and J.A. Planell, Formation of α-Widmanstätten Structure: Effects of Grain Size and Cooling Rate on the Widmanstätten Morphologies and on the Mechanical Properties in Ti6Al4V Alloy, *J. Alloys Compd.*, 2001, **329**, p 142–152
14. A. Dasgupta, T. Karthikeyan, S. Saroja, M. Vijayalakshmi, and V.S. Raghunathan, "Microstructural and microchemical investigations of Ti-5Ta-1.8Nb weldments using Analytical-TEM," *Proceedings of 58th IIM Annual Technical Meeting*, 2004, Trivananthapuram, India, p 234
15. A. Takamura, K. Arakawa, and Y. Moriguchi: "Corrosion Resistance of Titanium and Titanium-5% Tantalum Alloy in Hot Concentrated

Nitric Acid," *Proceedings on International Conference on Science Technology and Applications of Titanium*, R.I. Jaffee and N.E. Promisel, Eds., Pergamon Press, 1970, p 209–216

16. M. Metikos-Hukovic, A. Kwokal, and J. Piljac, The Influence of Niobium and Vanadium on Passivity of Titanium-based Implants in Physiological Solution, *Biomaterials*, 2003, **24**, p 3765–3775
17. R.W. Schutz and A.E. Thomas "Corrosion of Titanium and Titanium Alloys," *Metals Handbook*, ASM International, Ohio, USA, Vol. 13, 9th Ed., 1987, p 669–701
18. U. K. Mudali, R.K. Dayal, and J.B. Gnanamoorthy, Corrosion Behavior of Weldments of Ti and Ti-5Ta for Nuclear Fuel Reprocessing Plants, *J. Mater. Eng. Perform.*, 1995, **4**, p 756–760